Review Paper

Slip flow of Carreau fluid over a slendering stretching sheet with viscous dissipation and Joule heating

M. Gayatri[1] · K. Jayarami Reddy[1] · M. Jayachandra Babu[2]

Received: 27 September 2019 / Accepted: 13 February 2020 / Published online: 27 February 2020

Abstract
The effects of Joule heating and viscous dissipation on the two-dimensional Carreau fluid flowing through a stretching sheet with variable thickness are inspected with the supposition of slip parameters. The leading equations are altered as a set of (nonlinear) ordinary differential equations by means of proper similarity alterations. With the assistance of shooting procedure, subsequent equations are unravelled numerically. The impacts of appropriate parameters such as Weissenberg number and slip parameters (related to velocity and temperature) on the common profiles (velocity, concentration and temperature) are analysed via graphs. And also, we have analysed the effects of the identical parameters on skin friction coefficient and rate of transfers (heat and mass) by means of tables. From the outcomes, we observed that (a) the velocity slip parameter lowers the velocity but boosts the friction factor, (b) Weissenberg number boosts the velocity but shows conflicting behaviour on temperature, and (c) all boundary layers are observed to be thinner against wall thickness parameter. So, it benefits to improve both transfer rates (heat and mass), (d) the concentration boundary layer is observed to be thinner during chemical reaction, (e) magnetic field parameter and Eckert number are both reduce the local Nusselt number, and (f) wall thickness parameter and chemical reaction parameter are both improve the rate of mass transfer.

Keywords Joule heating · Viscous dissipation · Weissenberg number · Slip parameter · Shooting technique · Skin friction coefficient

1 Introduction

The no-slip boundary situation is acknowledged as the crucial rudiments of the Navier–Stokes theory. But there are circumstances wherein such condition is not proper. Mostly, no-slip condition is deficient for maximum non-Newtonian fluids. For illustration, polymer melts frequently show noticeable wall slip and that is denoted by a nonlinear and monotone fitting together amongst the slip velocity and traction. Moreover, partial velocity slips across a moving surface occur for fluids with particulate, for illustration, polymer solutions, emulsions, foams and suspensions. Firstly, Cohen and Metzner [1] demonstrated that the apparent slip phenomenon is an imperative feature of the flow behaviour of polymer solutions in inhomogeneous stress field. Lawal and Kalyon [2, 3] deliberated the wall slip in their study on the viscoelastic fluid flow amongst two parallel surfaces. They recognized the fact that the slip coefficient weakens the velocity gradient and substantially controls the temperature intensification. By considering stretching sheet, Ariel [4, 5] scrutinized the Newtonian and non-Newtonian fluid flows in the company of partial slip. He perceived that the flow gets hastened for distances close to the sheet upon the raise in viscoelastic fluid parameter. Fang et al. [6, 7] analytically resolved the equations which were raised in the work on the MHD fluid flow over a shrinking/stretching sheet.

✉ M. Gayatri, gayatri.mocherla@gmail.com | [1]Department of Mathematics, Koneru Lakshmaiah Education Foundation, Vaddeswaram, Andhra Pradesh, India. [2]Department of Mathematics, S.V.A. Govt. College, Srikalahasti, Andhra Pradesh, India.

They revealed that the wall slip velocity upsurges with the rise of magnetic field parameter. Zheng et al. [8] inspected the features of heat transfer on the stagnation point flow of nanofluids across a stretching sheet. One of their verdicts is that the thermophoresis and Brownian motion parameters both display the same impact on temperature. Rosca and Pop [9] did the stability analysis to display the twin solutions in their work on the two-dimensional viscous fluid flow across a vertical shrinking/stretching sheet. Malvandi et al. [10] and Ul Haq et al. [11] elucidated the impacts of (temperature and velocity) slip parameters on the stagnation point flow of nanofluid. Devi and Prakash [12] and Jayachandra Babu and Sandeep [13] analysed different MHD flows in the occurrence of slip parameters. Some of their detections are as follows: (a) temperature jump parameter lowers the temperature, and (b) wall thickness parameter lessens all the profiles (velocity, concentration and temperature). Mustafa [14] numerically deliberates the influence of slip parameters on nanofluid flow over a rotating disc. Usman et al. [15] and Ullah et al. [16] elucidated the slip effects on Casson fluid flow with viscous dissipation. They found the consequences: (a) thermal slip lowers the Nusselt number, and (b) viscous dissipation boosts the temperature. Abbas et al. [17] used Runge–Kutta–Fehlberg system to resolve the equations which were formulated in the work on the micropolar nanofluid flow near stagnation point. Recently, some researchers [18–22] deliberated various MHD flows in the slip regime.

When the plate is cooling or heating, the approximations of Joule heating and viscous dissipation are progressively noteworthy. The noticeable reality of heat transport naturally arises in the procedures of power generation systems, cooling of nuclear reactors, cooling of electronic chips or metallic sheets and liquid metal fluids. Firstly, Javeri [23] examined the effects of Joule heating and viscous dissipation on the MHD fluid flow along with Hall effect and ion slip. Later, Borisevich and Potanin [24] studied the heat transfer characteristics of incompressible fluid flow near a rotating disc. They observed that the temperature upsurges with the rise in the viscous dissipation. Mansour and Rama Subba Reddy [25] and Hakiem et al. [26] analysed the convective micropolar fluid flow with the same effects across different channels. They detected that the magnetic field parameter lowers the friction factor. Yih [27] employed implicit finite difference method to resolve the equations which were raised in the problem on the convective flow of non-Darcy fluid through a permeable sphere immersed in a porous medium. By considering the vertical surface, Chen [28] and Abo-Eldahad and Aziz [29] deliberated the heat transfer characteristics of two-dimensional fluid flow. One of their detections is that the Schmidt number improves the local Scherwood number. Osalusi et al. [30, 31] explained diverse MHD fluid flows through dissimilar channels. Some of their outcomes are as follows: (a) Hall parameter boosts the temperature, and (b) ion-slip current parameter rises the temperature. Later, several researchers [32–34] inspected various MHD flows including non-Newtonian fluid flow across various channels including a plane vertical channel. Jafar et al. [35] reported that the fluid temperature and velocity decreased with the increase in the shrinking of the sheet in their problem on the stagnation point flow through a shrinking/stretching surface. By keeping heat flux as constant, Haque et al. [36] and Chakraborty et al. [37] investigated the behaviour of various MHD fluid flows including micropolar fluid flow across narrow flow conduits. They saw that the temperature of the micropolar fluid is less for water contrast to air. Hayat et al. [38] employed HAM to solve the equations which were raised in the work on the unsteady MHD fluid flow across an exponentially stretching surface. Raju et al. [39] and Das et al. [40] deliberated convective MHD flows through porous medium. They revealed that the Prandtl number lowers the mean mixed temperature. Sheikholeslami and Ganji [41] utilized DTM to resolve the equations in the work on the scrutiny of nanofluids flow amongst two vertical permeable plates. They found that the shear stress decreases with the intensification of Lorentz forces. Recently, several researchers [42–44] contributed to the work on different flows accompanied with Ohmic (Joule) heating and viscous dissipation.

In this paper, the effects of Joule (Ohmic) heating, slip parameters and viscous dissipation on the two-dimensional Carreau fluid flowing through a stretching sheet with variable thickness are examined. Shooting technique is employed in this work to resolve the transmuted equations. To capture the changes and examine the common profiles (velocity, concentration and temperature) against several parameters together with viscous dissipation, plots were presented. And also, we have presented the physical values of friction factor, the rate of transfer (of both mass and heat) in the table for the same parameters. From the outcomes, it is found that velocity slip parameter lowers the velocity but boosts the friction factor, and Weissenberg number improves the velocity though displays reverse behaviour on temperature.

2 Mathematical formulation

A steady, laminar, incompressible, two-dimensional flow of non-Newtonian fluid (Carreau fluid) across a variable thickened stretching sheet is considered. The positive x-coordinate is measured along the direction of the moving sheet motion, and the positive y-coordinate is measured perpendicular to the sheet in the outward direction towards the fluid. We have applied a magnetic field of strength B_0 normal to the flow as shown in Fig. 1, which produces a magnetic effect in the x-direction. We assume that the stretching

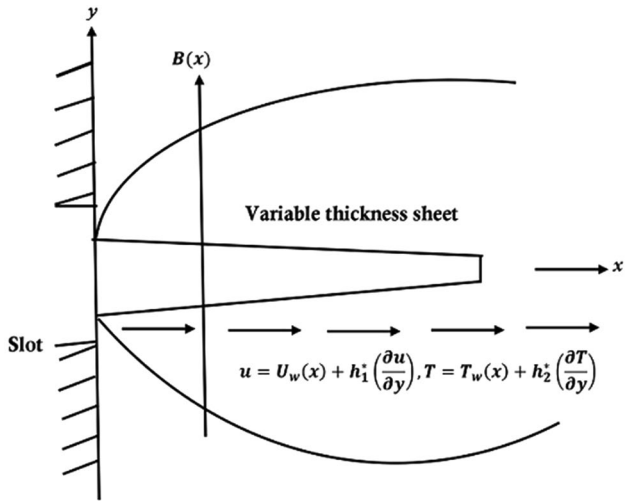

Fig. 1 Physical model of the problem

velocity is $U_w(x) = J_0(x+b)^m$ (J_0 is a constant and m is the velocity power index parameter). The sheet is not flat and is designated as $y = A(x+b)^{(1-m)/2}$, and the coefficient A is chosen as small for the sheet to be sufficiently thin, to avoid pressure gradient along the sheet $\left(\frac{\partial P}{\partial x} = 0\right)$. As we are considering stretching sheet with non-uniform thickness, this problem is valid for $m \neq 1$. The temperature and the concentration at the surface have constant values T_w and C_w, respectively. Hydrodynamic, thermal slip conditions are taken into the account at wall and Joule heating, and viscous dissipation effects are incorporated in the energy equation. Here magnetic field parameter is defined as $B(x) = B_0(x+b)^{\frac{m-1}{2}}$. Magnetic Reynolds number is presumed to be as fewer as possible in order to disregard the induced magnetic field. As the induced magnetic field is assumed to be negligible and since $B(x)$ is independent of time, $\text{curl}(\vec{E}) = 0$. In the absence of surface charge density, $\text{div}(\vec{E}) = 0$. Hence, the external electric field is assumed as negligible.

With these conditions, the leading equations [45] are

$$\frac{\partial u}{\partial x} + \frac{\partial v}{\partial y} = 0 \tag{1}$$

$$\begin{aligned} u\frac{\partial u}{\partial x} + v\frac{\partial u}{\partial y} &= \upsilon\frac{\partial^2 u}{\partial y^2}\left[1 + \Gamma^2\left(\frac{\partial u}{\partial y}\right)^2\right]^{\frac{n-1}{2}} \\ &+ \upsilon(n-1)\Gamma^2\frac{\partial^2 u}{\partial y^2}\left(\frac{\partial u}{\partial y}\right)^2\left[1 + \Gamma^2\left(\frac{\partial u}{\partial y}\right)^2\right]^{\frac{n-3}{2}} \\ &+ g\beta_T(T - T_\infty) + g\beta_C(C - C_\infty) - \frac{\sigma B^2(x)}{\rho}u \end{aligned} \tag{2}$$

$$u\frac{\partial T}{\partial x} + v\frac{\partial T}{\partial y} = \frac{k}{\rho c_p}\frac{\partial^2 T}{\partial y^2} + \frac{\sigma B^2(x)}{\rho c_p}u^2 + \frac{\upsilon}{c_p}\left(\frac{\partial u}{\partial y}\right)^2 \tag{3}$$

$$u\frac{\partial C}{\partial x} + v\frac{\partial C}{\partial y} = D_m\frac{\partial^2 C}{\partial y^2} - k_0(C - C_\infty) \tag{4}$$

and the matching boundary conditions are

$$\left.\begin{aligned} &u(x,y) = U_w(x) + h_1^*\left(\frac{\partial u}{\partial y}\right), v(x,y) = 0, T(x,y) = T_w(x) + h_2^*\left(\frac{\partial T}{\partial y}\right), \\ &C(x,y) = C_w(x) \quad \text{at } y = A(x+b)^{\frac{1-m}{2}} \\ &u(x,\infty) = 0, T(x,\infty) = T_\infty, C(x,\infty) = C_\infty \end{aligned}\right\} \tag{5}$$

where u, v are the velocity components in parallel to x- and y-directions, respectively, υ is the kinematic viscosity, Γ is the relaxation time of the Carreau fluid, n is the power law index parameter, g is the gravity field, β_T is the volumetric coefficient of thermal expansion, T_w is the surface temperature, β_C is the volumetric coefficient of diffusion expansion, σ is the electrical conductivity, ρ is the density of the fluid, $B(x)$ is the dimensional magnetic field parameter, k is the thermal conductivity, C_p is the specific heat capacitance, μ is the dynamic viscosity, C is the dimensional concentration parameter, D_m is the molecular diffusivity, k_0 is the dimensional chemical reaction parameter, h_1^* is the dimensional velocity slip parameter, and h_2^* is the dimensional temperature jump parameter.

Here $h_1^* = \left[\frac{2}{f_1} - 1\right]\xi_1(x+b)^{\frac{-m+1}{2}}$, $h_2^* = \left[\frac{2}{e} - 1\right]\xi_2(x+b)^{\frac{-m+1}{2}}$, $\xi_2 = \left(\frac{2\gamma}{1+\gamma}\right)\frac{\xi_1}{\text{Pr}}$, where f_1 is the Maxwell's reflection coefficient, ξ_1, ξ_2 are mean free path constants, e is the thermal accommodation coefficient, and γ is the ratio of specific heats.

The vital transmutations to alter the leading equations as (nonlinear coupled) ordinary differential equations are specified below:

$$\begin{aligned} \eta &= y\sqrt{\frac{m+1}{2}J_0\frac{(x+b)^{m-1}}{\upsilon}}, \\ u &= J_0(x+b)^m F'(\eta), \\ v &= -\sqrt{\frac{m+1}{2}\upsilon J_0(x+b)^{m-1}} \\ &\quad \left[F(\eta) + \left(\frac{m-1}{m+1}\right)\eta F'(\eta)\right], \\ \Theta(\eta) &= \frac{T - T_\infty}{T_w - T_\infty}, \Phi(\eta) = \frac{C - C_\infty}{C_w - C_\infty} \end{aligned} \tag{6}$$

By using (6), Eqs. (2)–(4) transmuted as the subsequent equations:

$$\frac{m+1}{2}\left[1+\mathrm{We}^2F''^2\right]^{\frac{n-3}{2}}\left[1+n\mathrm{We}^2F''^2\right]F''' + \frac{m+1}{2}FF'' - mF'^2 + \chi\Theta + \chi N^*\Phi - MF' = 0 \tag{7}$$

$$\Theta'' + \mathrm{Pr}\,F\Theta' + \frac{2}{m+1}M\,\mathrm{Pr}\,\mathrm{Ec}F'^2 + \mathrm{Pr}\,\mathrm{Ec}F''^2 = 0 \tag{8}$$

$$\Phi'' + \mathrm{Sc}F\Phi' - \frac{2}{m+1}ScKr\Phi = 0 \tag{9}$$

and the boundary conditions (5) altered as

$$\begin{aligned} &F(\lambda) = \frac{1-m}{1+m}\lambda\left[1+h_1F''(\lambda)\right], F'(\lambda) = 1+F''(\lambda),\\ &\Theta(\lambda) = 1+h_2\Theta'(\lambda), \Phi(\lambda) = 1,\\ &F'(\infty) = 0, \Theta(\infty) = 0, \Phi(\infty) = 0 \end{aligned} \tag{10}$$

where $\lambda = A\sqrt{\frac{J_0(m+1)}{2\upsilon}}$ is the wall thickness parameter.

Equations (7)–(9) can be transmuted into the system of dimensionless expressions with the help of the following:

$$\begin{aligned} &F(\eta) = f(\eta-\lambda) = f(\zeta),\\ &\Theta(\eta) = \theta(\eta-\lambda) = \theta(\zeta),\\ &\Phi(\eta) = \phi(\eta-\lambda) = \phi(\zeta) \end{aligned} \tag{11}$$

Then, the consequential equations are

$$\frac{m+1}{2}\left[1+\mathrm{We}^2f''^2\right]^{\frac{n-3}{2}}\left[1+n\mathrm{We}^2f''^2\right]f''' + \frac{m+1}{2}ff'' - mf'^2 + \chi\theta + \chi N^*\phi - Mf' = 0 \tag{12}$$

$$\theta'' + \mathrm{Pr}\,f\theta' + \frac{2}{m+1}M\,\mathrm{Pr}\,\mathrm{Ec}f'^2 + \mathrm{Pr}\,\mathrm{Ec}f''^2 = 0 \tag{13}$$

$$\phi'' + \mathrm{Sc}f\phi' - \frac{2}{m+1}\mathrm{ScKr}\phi = 0 \tag{14}$$

and the subsequent boundary conditions are

$$\begin{aligned} &f(0) = \frac{1-m}{1+m}\lambda\left[1+h_1f''(0)\right],\ f'(0) = 1+f''(0),\\ &\theta(0) = 1+h_2\theta'(0),\ \phi(0) = 1,\\ &f'(\infty) = 0, \theta(\infty) = 0,\ \phi(\infty) = 0 \end{aligned} \tag{15}$$

Here Weissenberg parameter We, mixed convection parameter χ, ratio of the concentration to the thermal buoyancy forces N^*, thermal Grashof number Gr, mass diffusion Grashof number Gc, Magnetic field parameter M, Eckert number, Prandtl number Pr, Schmidt number Sc, chemical reaction parameter Kr, h_1 velocity slip parameter and h_2 temperature jump parameter are defined as follows:

$$\begin{aligned} &\mathrm{We} = \left[\frac{J_0^3(m+1)\Gamma^2(x+b)^{3m-1}}{2\upsilon}\right]^{\frac{1}{2}}, \chi = \frac{Gr}{\mathrm{Re}_x^2}, N^* = \frac{Gc}{Gr},\\ &\mathrm{Gr} = \frac{g\beta_T\left(T_w-T_\infty\right)(x+b)^3}{\upsilon^2}, \mathrm{Gc} = \frac{g\beta_C\left(C_w-C_\infty\right)(x+b)^3}{\upsilon^2},\\ &M = \frac{\sigma B_0^2}{\rho J_0}, \mathrm{Pr} = \frac{\mu c_p}{k}, \mathrm{Ec} = \frac{U_w^2}{c_p\left(T_w-T_\infty\right)},\\ &\mathrm{Sc} = \frac{\upsilon}{D_m}, \mathrm{Kr} = \frac{k_0}{J_0(x+b)^{m-1}},\\ &h_1 = \left[\frac{2}{f_1}-1\right]\xi_1\sqrt{\frac{J_0(m+1)}{2\upsilon}},\\ &h_2 = \left[\frac{2}{e}-1\right]\xi_2\sqrt{\frac{J_0(m+1)}{2\upsilon}} \end{aligned} \tag{16}$$

The dimensional parameters of interest, local skin friction coefficient C_{fx}, the local Nusselt number Nu_x and the local Sherwood number Sh_x are defined as the following:

$$C_{f_x} = \frac{\tau_w}{\rho U_w^2(x)}, \mathrm{Nu}_x = \frac{(x+b)q_w}{k\left(T_w-T_\infty\right)}, \mathrm{Sh}_x = \frac{(x+b)q_m}{\left(C_w-C_\infty\right)} \tag{17}$$

where

$$\tau_w = \mu\frac{\partial u}{\partial y}\left[1+\Gamma^2\left(\frac{\partial u}{\partial y}\right)^2\right]^{\frac{n-1}{2}}\Bigg|_{y=A(x+b)^{\frac{1-m}{2}}},$$

$$q_w = -k\left(\frac{\partial T}{\partial y}\right)\Bigg|_{y=A(x+b)^{\frac{1-m}{2}}},$$

$$q_m = -D_m\left(\frac{\partial C}{\partial y}\right)\Bigg|_{y=A(x+b)^{\frac{1-m}{2}}}$$

With the help of (6) and (11), they can be transmuted as

$$\begin{aligned} &\left(\mathrm{Re}_x\right)^{1/2}C_{fx} = \sqrt{\frac{m+1}{2}}f''(0)\left[1+\mathrm{We}^2\left(f''(0)\right)^2\right]^{\frac{n-1}{2}},\\ &\left(\mathrm{Re}_x\right)^{-1/2}\mathrm{Nu}_x = -\sqrt{\frac{m+1}{2}}\theta'(0), \left(\mathrm{Re}_x\right)^{-1/2}Sh_x = -\sqrt{\frac{m+1}{2}}\phi'(0) \end{aligned} \tag{18}$$

where Re_x is defined as $\mathrm{Re}_x = \frac{U_w(x)(x+b)}{\upsilon}$

3 Numerical procedure

Numerical solutions of significantly nonlinear differential Eqs. (12)–(14) connected with the boundary conditions (15) are achieved with the aid of shooting procedure reliant on R–K fourth-order method.

Reduce Eqs. (12)–(14) into system of first-order equations by using sensible replacements described as follows:

$$\begin{aligned} f_1 &= f, \\ f_2 &= \frac{\mathrm{d}f_1}{\mathrm{d}\varsigma} = \frac{\mathrm{d}f}{\mathrm{d}\varsigma}, \\ f_3 &= \frac{\mathrm{d}f_2}{\mathrm{d}\varsigma} = \frac{\mathrm{d}^2 f}{\mathrm{d}\varsigma^2}, \\ f_4 &= \theta(\varsigma), \\ f_5 &= \frac{\mathrm{d}f_4}{\mathrm{d}\varsigma} = \frac{\mathrm{d}\theta}{\mathrm{d}\varsigma}, \\ f_6 &= \phi(\varsigma), \\ f_7 &= \frac{\mathrm{d}f_6}{\mathrm{d}\varsigma} = \frac{\mathrm{d}\phi}{\mathrm{d}\varsigma} \end{aligned} \tag{19}$$

By using this, we can write

$$\begin{aligned} \frac{\mathrm{d}f_1}{\mathrm{d}\zeta} &= f_2, \\ \frac{\mathrm{d}f_2}{\mathrm{d}\zeta} &= f_3, \\ \frac{\mathrm{d}f_3}{\mathrm{d}\zeta} &= -\frac{2}{[m+1]\left[1+\mathrm{We}^2 f_3\right]^{\frac{n-3}{2}}\left[1+n\mathrm{We}^2 f_3^2\right]} \\ &\quad \left[\frac{m+1}{2} f_1 f_3 - m f_2^2 + \chi f_4 + \chi N^* f_6 - M f_2\right] \\ \frac{\mathrm{d}f_4}{\mathrm{d}\zeta} &= f_5, \\ \frac{\mathrm{d}f_5}{\mathrm{d}\zeta} &= -\left[\mathrm{Pr}\, f_1 f_3 + \frac{2}{m+1} M\,\mathrm{Pr}\,\mathrm{Ec} f_2^2 + \mathrm{Pr}\,\mathrm{Ec} f_3^2\right], \\ \frac{\mathrm{d}f_6}{\mathrm{d}\zeta} &= f_7, \\ \frac{\mathrm{d}f_7}{\mathrm{d}\zeta} &= \frac{2}{m+1}\mathrm{Sc}\,\mathrm{Kr} f_6 - \mathrm{Sc} f_1 f_7 \end{aligned} \tag{20}$$

We can use an analogous approach for the boundary conditions stated in (15). After the alteration, we can employ the shooting procedure dependent on R–K fourth-order method to get the reasonable results. The boundary conditions $f\prime(0), \theta(0)$ and $\phi(0)$ for $\zeta \to \infty$ are altered into finite interval length ($\zeta = 5$). Insert three primary suppositions to $f''(0), \theta'(0)$ and $\phi'(0)$ for probable solution. Here the step size and convergence criteria are chosen to be 0.001 and 10^{-6} (in all cases).

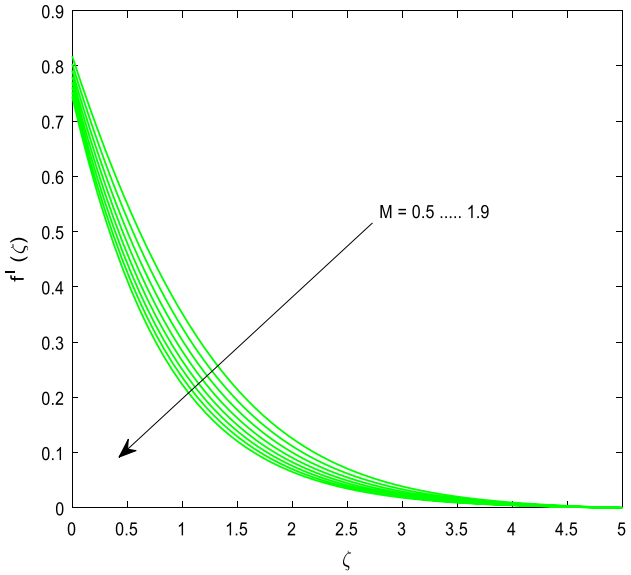

Fig. 2 Influence of M on velocity profile

4 Results and Discussion

The set of (ordinary differential) Eqs. (12)–(14) with respect to the boundary conditions (15) is solved numerically by applying R–K fourth-order-based shooting procedure. We exhibited the impact of non-dimensional parameters, for example We, Ec, h_1 on velocity, concentration and temperature, using plots and the impact of the same parameters on friction factor, rate of transfer (both mass and heat) using tables.

Figure 2 shows the impact of M on velocity profile. It is evident from the figure that M lowers the velocity. This occurs because of Lorentz force emerging from the collaboration of electric and magnetic fields during the movement of an electrically conducting fluid. The produced Lorentz force controls the fluid movement in boundary layer area and thus lessening the thickness of the momentum boundary layer. So, velocity diminishes with the rise in M. Because of the mounting of Lorentz force, thickness of the thermal boundary layer upsurges. As a consequence, temperature increases with the increase in M which can be observed in Fig. 3. When we increase We, there is a diminution in the viscosity of the fluid. So, with the rise in We, there is an enhancement in the velocity (Fig. 4) and drop in the temperature (Fig. 5). From the Fig. 6, we can observe that Ec raises the temperature. Generally, when we increase Ec, additional heat will be added to the fluid flow. As

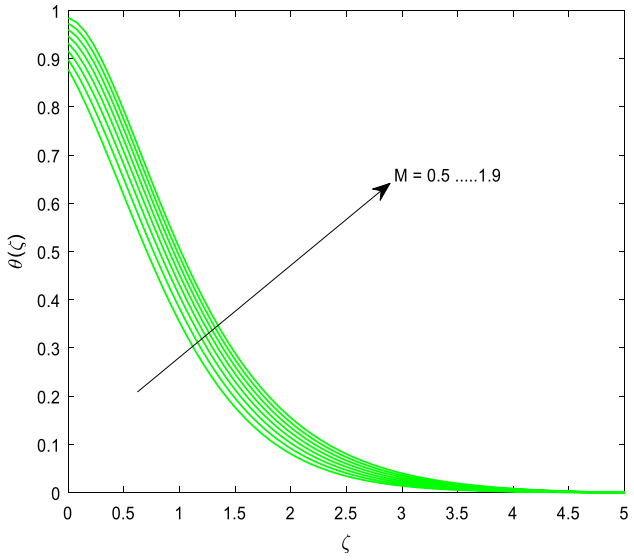

Fig. 3 Influence of *M* on temperature profile

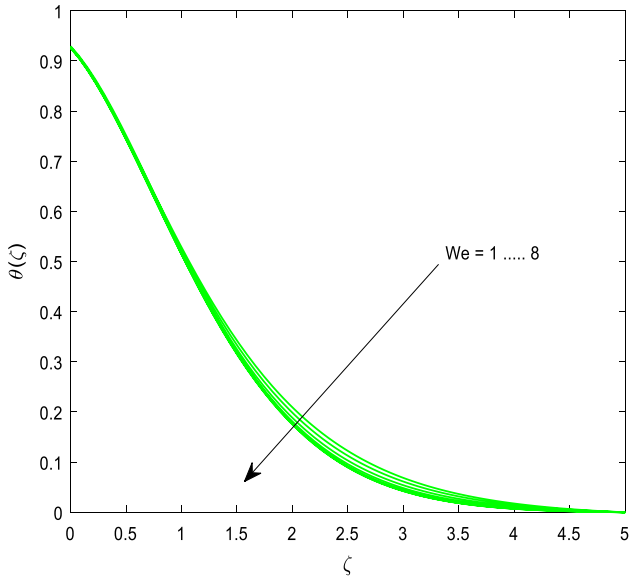

Fig. 5 Influence of We on temperature profile

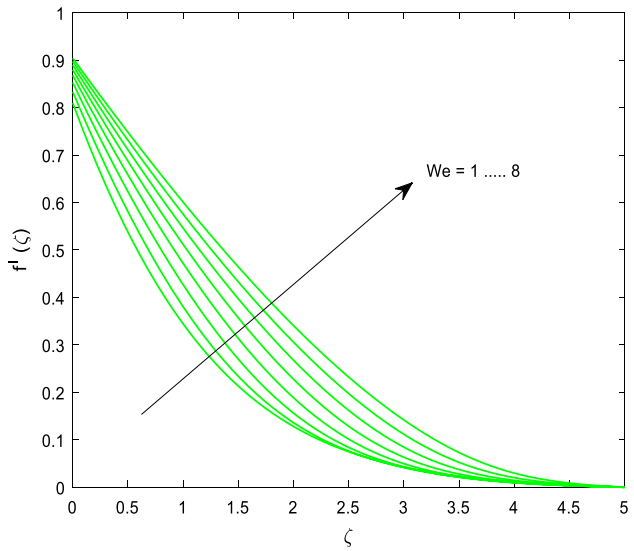

Fig. 4 Influence of We on velocity profile

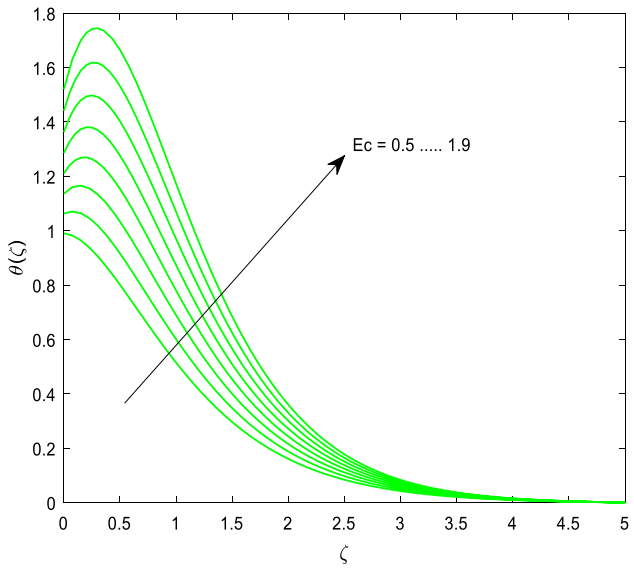

Fig. 6 Influence of Ec on temperature profile

a result, temperature increases. Figure 7 explained the fact that χ boosts the velocity profile. This may be due to the fact that the increase in χ leads to the diminution in the density of the fluid. We know the fact that Sc is inversely proportional to the mass diffusion. So, when we increase Sc, there is a reduction in the concentration profile (Fig. 8). Figure 9 shows the natural behaviour of Kr on the concentration. Figures 10 and 11 revealed the influence of λ on velocity and temperature profiles. From these, we can notice that λ lessens all profiles. Reasons behind this behaviour may be the following: (a) increasing λ barricades the flow motion to slow down the flow field. Eventually, the boundary layer thickness gets thinner for increasing values of λ, and (b) thicker surfaces slowly emit the heat into the flow. So, when we increase λ, there is a reduction in the heat dissipation towards the

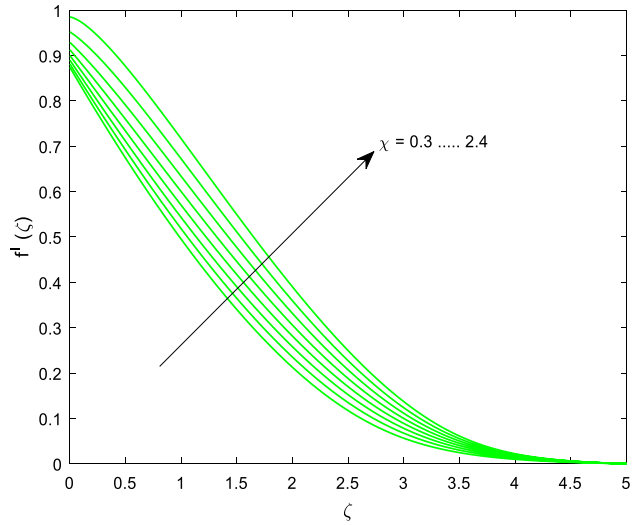

Fig. 7 Influence of χ on velocity profile

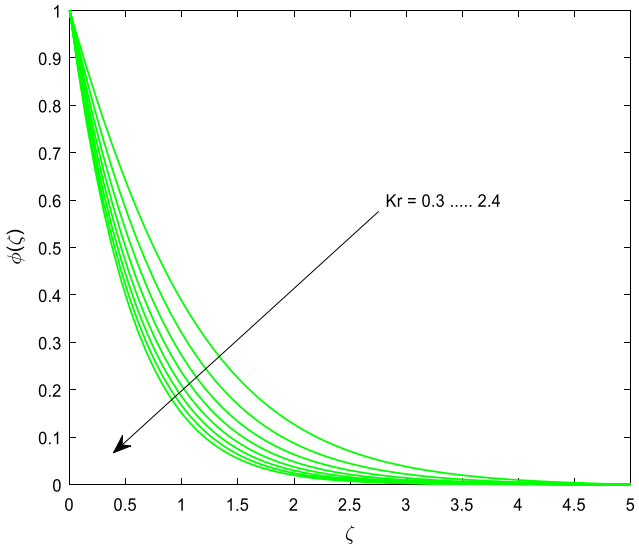

Fig. 9 Influence of Kr on concentration profile

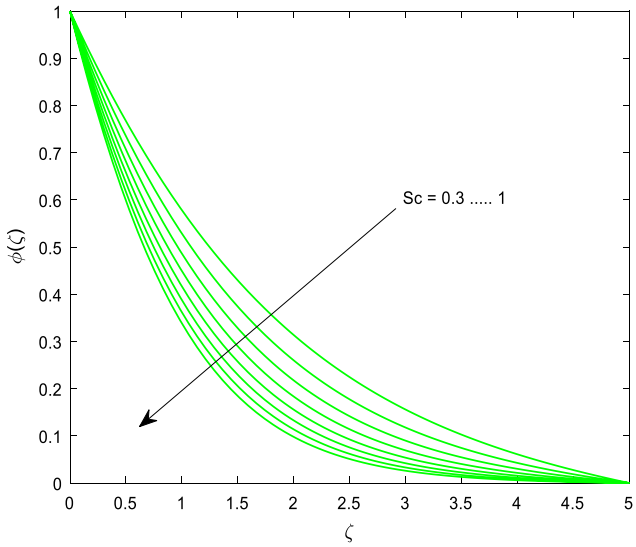

Fig. 8 Influence of Sc on concentration profile

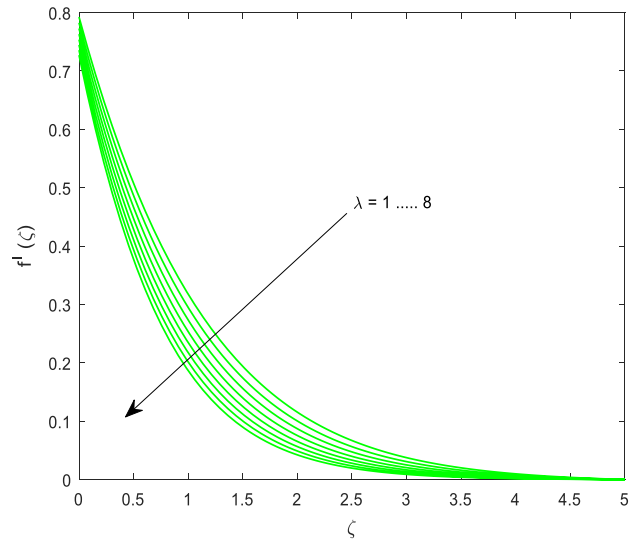

Fig. 10 Influence of λ velocity on profile

flow which causes the reduction in temperature. From Fig. 12, we can notice that h_1 lessens the velocity. When we increase h_1, initially velocity gets decreased near the surface the sheet and ultimately, in the entire fluid flow, velocity decreases. When we increase h_2, thermal accommodation coefficient upsurges which lowers the thermal diffusion towards the flow. So, temperature decreases with the rise in h_2 (Fig. 13). Table 1 displays the values of local skin friction coefficient and rate of transfers (heat and mass) against the aforesaid parameters. *We* and h_1 are beneficial to improve the friction factor, rate of transfers (heat and mass). *M* and Ec both lessen the heat transfer rate. λ and Kr both improve the rate of mass transfer. Table 2 displays the assessment of the present result with the existing results in the restrictive case. We found decent agreement.

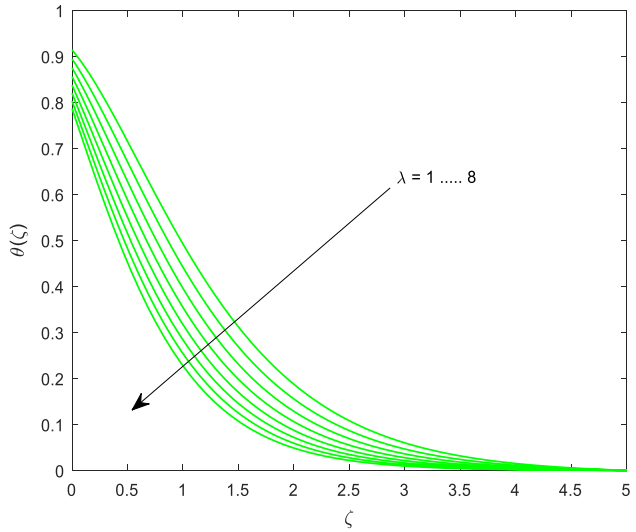

Fig. 11 Influence of λ temperature on profile

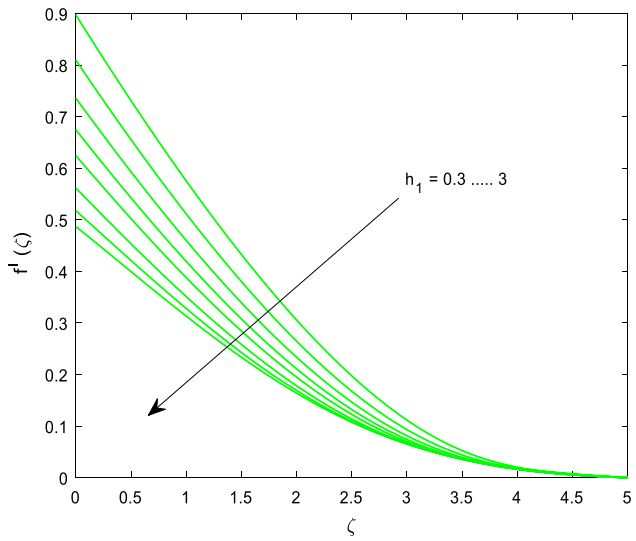

Fig. 12 Influence of h_1 on velocity profile

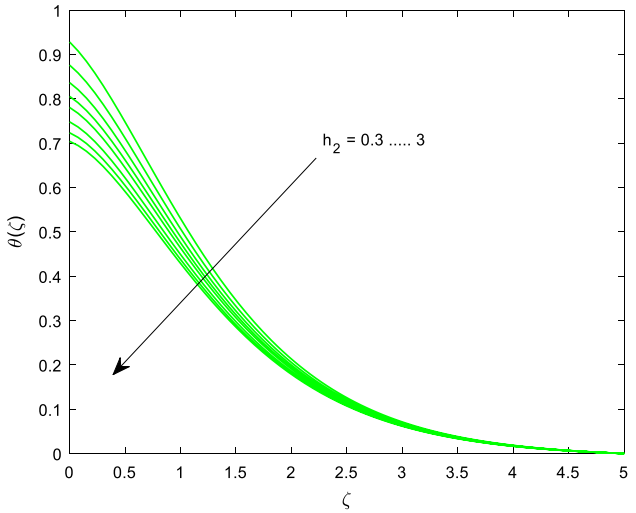

Fig. 13 Influence of h_2 on temperature profile

5 Conclusions

When the plate is cooling or heating, the estimations of Joule heating and viscous dissipation are progressively significant. The noticeable reality of heat transport typically emerges in the procedures of power generation systems, cooling of nuclear reactors, cooling of electronic chips or metallic sheets and liquid metal fluids. Keeping these facts in the mind, the current study addresses the convective flow of Carreau fluid across a slendering stretching sheet in the presence of Joule heating, viscous dissipation and slip parameters. Numerical solutions of altered equations are achieved via shooting technique. The impacts of various parameters including viscous dissipation on the usual profiles (velocity, concentration and temperature) deliberated and demonstrated by means of plots. The effects of same parameters on the friction factor, rate of transfers (heat and mass) are conversed via Table 1. We also utilized special occurrences of the present model to approve our outcomes with past inquiries (Table 2). The subsequent deductions can be drawn from the present study.

- We improves the velocity and lessen the temperature
- All boundary layers are observed to be thinner against λ. So, it benefits to improve both transfer rates (heat and mass).
- h_1 lowers the velocity and boosts the friction factor.
- The concentration boundary layer is observed to be thinner during chemical reaction.

Table 1 Amounts of skin friction coefficient and transfer rates (heat and mass) for various parameters

We	M	Ec	λ	h_1	h_2	Kr	C_{f_x}	Nu_x	Sh_x
1							−0.634262	0.240165	0.961156
2							−0.555918	0.242368	0.973793
3							−0.490994	0.245680	0.986506
	1						−0.668549	0.240240	0.956555
	2						−0.854700	0.090321	0.926272
	3						−0.989458	−0.996421	0.905473
		0.5					−0.668549	0.240240	0.956555
		1					−0.642746	−0.045985	0.962072
		1.5					−0.615436	−0.343435	0.967882
			1				−0.691891	0.286642	0.999353
			2				−0.725008	0.352552	1.061548
			3				−0.757682	0.417414	1.124794
				0.3			−0.668549	0.240240	0.956555
				0.6			−0.507252	0.278472	0.936039
				0.9			−0.408397	0.296612	0.923622
					0.3		−0.668549	0.240240	0.956555
					0.6		−0.675122	0.206953	0.955424
					0.9		−0.680118	0.181857	0.954561
						0.3	−0.662017	0.242314	0.823757
						0.6	−0.671266	0.239396	1.016331
						0.9	−0.677959	0.237386	1.177094

Table 2 Comparison of local Nusselt number for various values of Pr when $M = \mathrm{Ec} = h_1 = h_2 = \mathrm{Le} = \chi = N^* = 0, \mathrm{We} = 3, m = 1, n = 0.5$

Pr	Local Nusselt number $(-\theta'(0))$	
	Khan and Hashim [45]	Present study
0.5	0.322215	0.326430
1	0.524684	0.525073
1.5	0.691768	0.691736
2	0.835148	0.835092

- M and Ec both reduce the local Nusselt number. λ and Kr both improve the rate of mass transfer.

Compliance with ethical standards

Conflict of interest On behalf of all authors, the corresponding author states that there is no conflict of interest.

References

1. Cohen Y, Metzner AB (1985) Apparent slip flow of polymer solutions. J Rheol 29:67. https://doi.org/10.1122/1.549811
2. Lawal A, Kalyon DM (1997) Nonisothermal extrusion flow of viscoplastic fluids with wall slip. Int J Heat Mass Transf 40(16):3883–3897. https://doi.org/10.1016/S0017-9310(97)00016-1
3. Lawal A, Kalyon DM (1998) Squeezing flow of viscoelastic fluids subjects to wall slip. Polym Eng Sci 38(11):1793–1804. https://doi.org/10.1002/pen.10349
4. Ariel PD (2006) The flow of an elastic-viscous fluid past a stretching sheet with partial slip. Acta Mech 187:29–35. https://doi.org/10.1007/s00707-006-0370-3
5. Ariel PD (2007) Axisymmetric flow due to a stretching sheet with partial slip. Comput Math Appl 54:1169–1183. https://doi.org/10.1016/j.camwa.2006.12.063
6. Fang T, Zhang Ji, Yao S (2009) Slip MHD viscous flow over a stretching sheet—an exact solution. Commun Nonlinear Sci Numer Simul 14:3731–3737. https://doi.org/10.1016/j.cnsns.2009.02.012
7. Fang T, Yao S, Zhang Ji, Aziz A (2010) Viscous flow over a shrinking sheet with a second order slip flow model. Commun Nonlinear Sci Numer Simul 15:1831–1842. https://doi.org/10.1016/j.cnsns.2009.07.017
8. Zheng L, Zhang C, Zhang X, Zhang J (2013) Flow and radiation heat transfer of a nanofluids over a stretching sheet with velocity slip and temperature jump in porous medium. J Franklin Inst 350:990–1007. https://doi.org/10.1016/j.jfranklin.2013.01.022
9. Rosca AV, Pop I (2013) Flow and heat transfer over a vertical permeable stretching/shrinking sheet with a second order slip. Int J Heat Mass Transf 60:355–364. https://doi.org/10.1016/j.ijheatmasstransfer.2012.12.028
10. Malvandi A, Hedayati F, Ganji DD (2014) Slip effects on unsteady stagnation point flow of a nanofluids over a stretching sheet. Powder Technol 253:377–384. https://doi.org/10.1016/j.powtec.2013.11.049

11. Ul Haq R, Nadeem S, Khan ZH, Akbar NS (2015) Thermal radiation and slip effects on MHD stagnation point flow of nanofluid over a stretching sheet. Physica E 65:17–23. https://doi.org/10.1016/j.physe.2014.07.013
12. Devi SP, Prakash M (2016) Slip flow effects over hydromagnetic forced convective flow over a slendering stretching sheet. J Appl Fluid Mech 9(2):683–692
13. Jayachandra Babu M, Sandeep N (2016) Three-dimensional MHD slip flow of nanofluids over a slendering stretching sheet with thermophoresis and Brownian motion effects. Adv Powder Technol 27(5):2039–2050. https://doi.org/10.1016/j.apt.2016.07.013
14. Mustafa M (2017) MHD nanofluid flow over a rotating disk with partial slip effects: Buongiorno model. Int J Heat Mass Transf 108:1910–1916. https://doi.org/10.1016/j.ijheatmasstransfer.2017.01.064
15. Usman M, Soomro FA, Ul Haq R, Wang W, Defterli O (2018) Thermal and velocity slip effects on Casson nanofluids flow over an inclined permeable stretching cylinder via collocation method. Int J Heat Mass Transf 122:1255–1263. https://doi.org/10.1016/j.ijheatmasstransfer.2018.02.045
16. Ullah I, Alkanhal TA, Shafie S, Nisar KS, Khan I, Makinde OD (2019) MHD slip flow of Casson fluid along a nonlinear permeable stretching cylinder saturated in a porous medium with chemical reaction, viscous dissipation, and heat generation/absorption. Symmetry 11(4):531. https://doi.org/10.3390/sym11040531
17. Abbas N, Saleem S, Nadeem S, Alderremy AA, Khan AU (2018) On stagnation point flow of a micro polar nanofluids past a circular cylinder with velocity and thermal slip. Results Phys 9:1224–1232. https://doi.org/10.1016/j.rinp.2018.04.017
18. Sampath Kumar PB, Gireesha BJ, Mahanthesh B, Chamkha AJ (2019) Thermal analysis of nanofluid flow containing gyrotactic microorganisms in bioconvection and second-order slip with convective condition. J Therm Anal Calorim 136(5):1947–1957. https://doi.org/10.1007/s10973-018-7860-0
19. Basma S, Ganesh Kumar K, Gnaneswara Reddy M, Rani Sudha, Najib H, Huda A, Mohammad RG (2019) Slip flow and radiative heat transfer behavior of Titanium alloy and ferromagnetic nanoparticles along with suspension of dusty fluid. J Mol Liq 290:111223. https://doi.org/10.1016/j.molliq.2019.111223
20. Durga Prasad P, Saleem S, Varma SVK, Raju CSK (2019) Three dimensional slip flow of a chemically reacting Casson fluid flowing over a porous slender sheet with a non-uniform heat source or sink. J Korean Phys Soc 74(9):855–864. https://doi.org/10.3938/jkps.74.855
21. Hamid M, Zubair T, Usman M, Khan ZH, Wang W (2019) Natural convection effects on heat and mass transfer of slip flow of time-dependent Prandtl fluid. J Comput Design Eng 6:584–592. https://doi.org/10.1016/j.jcde.2019.03.004
22. Krishna Murthy M, Raju CSK, Nagendramma V, Shehzad SA, Chamkha AJ (2019) Magnetohydrodynamics boundary layer slip Casson fluid flow over a dissipated stretched cylinder. Defect Diffus Forum 393:73–82. https://doi.org/10.4028/www.scientific.net/DDF.393.73
23. Javeri V (1975) Combined influence of Hall effect, ion slip, viscous dissipation and joule heating on MHD heat transfer in a channel. Warme-und stoffubertragung 8:193–202. https://doi.org/10.1007/BF01681561
24. Borisevich VD, Potanin EP (1988) Effects of viscous dissipation and joule heat on heat transfer near a rotating disk in the presence of intensive suction. Moscow Eng Phys Inst 55(5):740–743. https://doi.org/10.1007/BF00872613
25. Mansour MA, Rama Subba Reddy G (1998) Joule-heating effects on unsteady natural convection from a heated vertical plate in a micropolar fluid. Can J Phys 76:977–984. https://doi.org/10.1139/p98-069
26. El-Hakiem MA, Mohammadein AA, El-Kabeir SMM, Rama Subba Reddy G (1999) Joule heating effects on magnetohydrodynamic free convection flow of a micropolar fluid. Int Commun Heat Mass Transf 26(2):219–227. https://doi.org/10.1016/S0735-1933(99)00008-1
27. Yih KA (2000) Viscous and joule heating effects on non-Darcy MHD natural convection flow over a permeable sphere in porous media with internal heat generation. Int Commun Heat Mass Transf 27(4):591–600. https://doi.org/10.1016/S0735-1933(00)00141-X
28. Chen Chien-Hsin (2004) Combined heat and mass transfer in MHD free convection from a vertical surface with Ohmic heating and viscous dissipation. Int J Eng Sci 42:699–713. https://doi.org/10.1016/j.ijengsci.2003.09.002
29. Abo-Eldahad EM, El Aziz MA (2005) Viscous dissipation and joule heating effects on MHD free convection from a vertical plate with power-law variation in surface temperature in the presence of Hall and ion-slip currents. Appl Math Model 29:579–595. https://doi.org/10.1016/j.apm.2004.10.005
30. Osalusi E, Side J, Harris R, Johnston B (2007) On the effectiveness of viscous dissipation and Joule heating on steady MHD flow and heat transfer of a Bingham fluid over a porous rotating disk in the presence of Hall and ion-slip currents. Int Commun Heat Mass Transfer 34:1030–1040. https://doi.org/10.1016/j.icheatmasstransfer.2007.05.008
31. Osalusi E, Side J, Harris R, Clark P (2008) The effect of combined viscous dissipation and Joule heating on unsteady mixed convection MHD flow on a rotating cone in a rotating fluid with variable properties in the presence of Hall and ion-slip currents. Int Commun Heat Mass Transf 35:413–429. https://doi.org/10.1016/j.icheatmasstransfer.2007.09.002
32. Barletta A, Celli M (2008) Mixed convection MHD flow in a vertical channel: Effects of Joule heating and viscous dissipation. Int J Heat Mass Transf 51:6110–6117. https://doi.org/10.1016/j.ijheatmasstransfer.2008.04.009
33. Sahoo B (2009) Effects of partial slip, viscous dissipation and Joule heating on Von Karman flow and heat transfer of an electrically conducting non-Newtonian fluid. Commun Nonlinear Sci Numer Simul 14:2982–2998. https://doi.org/10.1016/j.cnsns.2008.10.021
34. Alam MS, Rahman MM, Sattar MA (2009) On the effectiveness of viscous dissipation and Joule heating on steady magnetohydrodynamic heat and mass transfer flow over an inclined radiate isothermal permeable surface in the presence of thermophoresis. Commun Nonlinear Sci Numer Simul 14:2132–2143. https://doi.org/10.1016/j.cnsns.2008.06.008
35. Jafar K, Nazar R, Ishak A, Pop I (2011) Stretching/shrinking sheets with external field, viscous dissipation and Joule effects. Can J Chem Eng 9999:1–11. https://doi.org/10.1002/cjce.20609
36. Haque MZ, Alam MM, Ferdows M, Postelnicu A (2012) Micropolar fluid behaviours on steady MHD free convection and mass transfer flow with constant heat and mass fluxes, joule heating and viscous dissipation. J Kind Saud Univ Eng Sci 24:71–84. https://doi.org/10.1016/j.jksues.2011.02.003
37. Chakraborty R, Dey R, Chakraborty S (2013) Thermal characteristics of electromagnetohydrodynamic flows in narrow channels with viscous dissipation and Joule heating under constant wall heat flux. Int J Heat Mass Transf 67:1151–1162. https://doi.org/10.1016/j.ijheatmasstransfer.2013.08.099
38. Hayat T, Naseem A, Farooq M, Alsaedi A (2013) Unsteady MHD three-dimensional flow with viscous dissipation and Joule heating. Eur Phys J Plus 128(12):158. https://doi.org/10.1140/epjp/i2013-13158-1

39. Raju KVS, Sudhakar Reddy T, Raju MC, Satya Narayana PV, Venkataramana S (2014) MHD convective flow through porous medium in a horizontal channel with insulated and impermeable bottom wall in the presence of viscous dissipation and Joule heating. Ain Shams Eng J 5:543–551. https://doi.org/10.1016/j.asej.2013.10.007
40. Das S, Jana RN, Makinde OD (2015) Magnetohydrodynamic mixed convective slip flow over an inclined porous plate with viscous dissipation and Joule heating. Alex Eng J 54:251–261. https://doi.org/10.1016/j.aej.2015.03.003
41. Sheikholeslai M, Ganji DD (2016) Nanofluid hydrothermal behavior in existence of Lorentz forces considering Joule heating effect. J Mol Liq 224:526–537. https://doi.org/10.1016/j.molliq.2016.10.037
42. Ganesh Kumar K, Ramesh GK, Gireesha BJ, Gorla RSR (2018) Characteristics of Joule heating and viscous dissipation on three-dimensional flow of Oldroyd B nanofluids with thermal radiation. Alex Eng J 57:2139–2149. https://doi.org/10.1016/j.aej.2017.06.006
43. Pordanjani AH, Raisi A, Ghasemi B (2019) Numerical simulation of the magnetic field and Joule heating effects on force convection flow through parallel plate microchannel in the presence of viscous dissipation effect. Numer Heat Transf Part A: Appl 76(6):499–516. https://doi.org/10.1080/10407782.2019.1642053
44. Lalami AA, Afrouzi HH, Moshfegh A, Omidi M, Javadzadegan A (2019) Investigation of nanofluids heat transfer in a microchannel under magnetic field via lattice Boltzmann method: effects of surface hydrophobicity, viscous dissipation and Joule heating. J Heat Transf 141(6):062403. https://doi.org/10.1115/1.4043163
45. Khan M, Hashim (2015) Boundary layer flow and heat transfer to Carreau fluid over a nonlinear stretching sheet. AIP Adv 5(10):107203. https://doi.org/10.1063/1.4932627